DOI: 10.1002/ejic.200600215

Study of the In Situ Postintercalative Polymerization of Metanilic Anions Intercalated in NiAl-Layered Double Hydroxides under a Nitrogen Atmosphere

Min Wei,[a] Xiaofei Tian,[a] Jing He,[a] Min Pu,[a] Guoying Rao,[a] Heli Yang,[a] Lan Yang,[a] Tao Liu,[b] David G. Evans,[a] and Xue Duan*[a]

Keywords: In situ polymerization / Polyaniline / Layered double hydroxides / Nitrogen atmosphere

A new route has been developed for preparing polyaniline (PANI) layered double hydroxide (LDH) nanocomposites through in situ chemical oxidative polymerization of metanilic anions (m-$NH_2C_6H_4SO_3^-$) intercalated in NiAl LDHs under a nitrogen atmosphere by using pre-intercalated nitrate as an oxidizing agent. The interlayer space of NiAl LDHs has been used as an original nanoreactor for the in situ polymerization of the intercalated monomer. The whole process involves the synthesis of the precursor LDH [$Ni_2Al(OH)_6(NO_3)\cdot nH_2O$], the intercalation of the monomer metanilic anions into the LDH and its in situ polymerization between the layers by thermal treatment under a nitrogen atmosphere. The interlayer polymerization reaction was monitored by thermogravimetric analysis (TG), differential thermal analysis (DTA), mass spectrometry (MS), UV/Vis absorption spectroscopy, in situ X-ray absorption near edge structure (XANES) spectroscopy, in situ high-temperature X-ray diffraction (HT-XRD) and in situ Fourier transform infrared (FTIR) spectroscopy. The UV/Vis spectra provide evidence for the polymerization of the intercalated metanilic anions, and an increase in the interlayer distance from 16.0 to 17.2 Å is observed by HT-XRD. It has been found by the in situ techniques that the pre-intercalated nitrate anions act as the oxidizing agent that induces the polymerization of the interlayer monomer under a nitrogen atmosphere upon heating at 300 °C. The orientation of the interlayer polymerization product has also been proposed.

Introduction

In recent years, considerable interest has been devoted to nanocomposites prepared from the assembly of an organic polymer and an inorganic layered material. Polymer intercalation nanocomposites prepared by using layered materials are expected to consist of a high degree of polymeric ordering and to exhibit advanced physicochemical properties compared with the individual parts.[1–5]

Among the organic polymers, polyaniline (PANI) has been and continues to be extensively studied as an organic component in such systems. Polyaniline is a promising conjugated polymer because of its simple synthesis, high conductivity, and excellent environmental stability, although it is associated with rather poor properties with respect to processing. Consequently, there are many reports focusing on the preparation of novel nanocomposites consisting of PANI with various layered materials such as V_2O_5 xerogel,[6] MoO_3 bronze,[7] graphitic oxide,[8] α-$RuCl_3$,[9] montmorillonite,[10] and layered metal phosphates.[11]

As for the layered materials, LDHs have received considerable attention because of their special intercalation properties. LDHs, which are widely known as a class of anionic clays, can be represented by the general formula $[M_{1-x}^{II}M_x^{III}(OH)_2]^{x+}(A^{n-})_{x/n}\cdot mH_2O$, where M^{II} and M^{III} are divalent and trivalent metal cations, respectively. A^{n-} is an exchangeable inorganic or organic anion and the x value, i.e. the charge density, is equal to the molar ratio $M^{III}/(M^{III} + M^{II})$. LDHs have positively charged layers, and a wide variety of charge-balancing anionic species have been intercalated into the gallery region.[12] As a result, LDHs are now well established as excellent anion-exchange materials and their extensive intercalation chemistry has widespread applications in the area of organic/inorganic nanocomposites.[13]

PANI/LDH nanocomposites were first reported by Challier and Slade.[14] Prior to the incorporation, the LDH host structure was exchanged with terephthalate or hexacyanoferrate anions in order to expand the basal spacing. The pre-swollen LDH materials were then heated at reflux with pure aniline. Analysis of the XRD patterns of the products confirmed the presence of multiple phases. More recently, interlayer polymerization methods have concentrated on heat treatment after polymeric monomer intercalation into the LDH. This process is the so called "soft thermal treatment", which is a two-step soft chemistry route that in-

[a] State Key Laboratory of Chemical Resource Engineering, Beijing University of Chemical Technology, Beijing 100029, P. R. China
[b] Institute of High Energy Physics, Chinese Academy of Science, Beijing 100039, P. R. China
E-mail: duanx@mail.buct.edu.cn

cludes the intercalation of aniline sulfonic acid between the sheets of the LDHs and its subsequent in situ polymerization at a temperature below 200 °C in air. This approach can avoid the ion-exchange reaction competing with the interlayer polymerization as well as the destruction of the layered structure by external oxidizing agents. As in the case of other lamellar nanocomposites, atmospheric oxygen was found to play a major role in the polymerization process.[15–17]

In the present study, we report a new route for preparing PANI/LDH nanocomposites by using pre-intercalated nitrates as the oxidizing agent. In situ chemical oxidative polymerization of metanilic anions (m-$NH_2C_6H_4SO_3^-$) intercalated in NiAl LDHs under a nitrogen atmosphere has been performed for the first time. The whole process involves the synthesis of the precursor LDH [$Ni_2Al(OH)_6(NO_3)\cdot nH_2O$], the intercalation of the monomer metanilic anions into the LDH and its in situ polymerization between the layers by thermal treatment under nitrogen. Advantages of this method are: (1) the restricted interlayer region of the LDH makes it easier to obtain nanosized oligomers with uniform size; (2) the pre-intercalated NO_3^- acting as an oxidizing agent can prevent the influence of mass transfer and diffusion on the polymerization reaction of the interlayer monomer. A combination of techniques, including TG–DTA–MS, UV/Vis, in situ XANES, in situ HT-XRD, and in situ FTIR spectroscopy, was used for the characterization of intercalated metanilic anions and their in situ interlayer polymerization. UV/Vis spectroscopy provides evidence for the polymerization of the intercalated monomer, and an increase in the interlayer distance from 16.0 to 17.3 Å is observed by HT-XRD. It has been found by the in situ techniques that the pre-intercalated nitrate anions act as the oxidizing agent, which induces the polymerization of the interlayer monomer upon heating at 300 °C under nitrogen. The orientation of the interlayer polymerization product has also been proposed.

Results and Discussion

Structure of NiAl-Metanilic LDHs

The X-ray diffraction patterns of the precursor NiAl-NO_3 LDH and the metanilic anion intercalated LDH are shown in Figure 1. In each case, the reflections can be indexed to a hexagonal lattice with R-3m rhombohedral symmetry, commonly used for the description of the LDH structures.[19] The main diffraction peaks for NiAl-NO_3 LDH appear at 9.9° (003), 19.9° (006), 29.5° (009), and 62.1° (110) (Figure 1a), while the corresponding peaks for NiAl-metanilic LDH are observed at 5.4°, 11.1°, 16.8°, and 61.7° (Figure 1b), respectively. Apparently, the XRD pattern for NiAl-metanilic LDH exhibits the characteristic reflections of LDH materials with a series of (00l) peaks, which are evidence for the layered character. The interlayer distance for the NiAl-NO_3 LDH is 8.9 Å which is larger than that reported by Prinetto et al. (8.3 Å, for the existence of a large amount of CO_3^{2-}).[20] After the intercalation of metanilic acid, the value of the interlayer distance increased to 16.3 Å, which is 7.4 Å larger than that of NiAl-NO_3 LDH. The expansion of the basal spacing was due to the intercalation of metanilic anions into the LDH lamellar. Thus, the interaction of NiAl-NO_3 LDH with an aqueous solution of metanilic acid at pH 7.0 led to the anion exchange of NO_3^- for the metanilic anions with conservation of the layered structure. As for the (110) reflection, no obvious shift was observed after intercalation, indicating that no significant change occurred in the LDH layer.

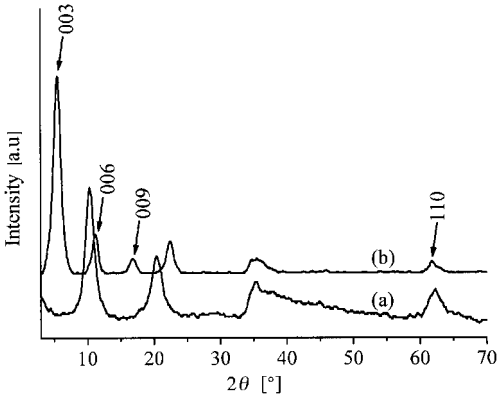

Figure 1. XRD patterns for (a) NiAl-NO_3 LDH and (b) NiAl-metanilic LDH.

The size of the gallery height of 11.5 Å, obtained by subtracting the thickness of the aluminium hydroxide layer (4.8 Å) from the interlayer distance (16.3 Å),[21] was much longer than a single perpendicular anion height (6.4 Å, calculated with Chemwin 6.0) but shorter than its double value. This may indicate that the guest anions are accommodated with an interpenetrating arrangement, leaving interstitial gaps between the monomers and the hydroxide sheets. Water molecules and nitrate anions occupy these interstitial spaces.

Compared with the NiAl-NO_3 LDH precursor (Figure 2a), three strong bands at 1599, 1484, and 1454 cm^{-1} and two weak bands at 1257 and 1315 cm^{-1} are observed in the FTIR spectrum of NiAl-metanilic LDH (Figure 2b), which can be attributed to the characteristic absorptions of metanilic anions.[22] The remarkable absorption band at 1384 cm^{-1} resulting from the stretching vibration of NO_3^- is also observed. It can be seen that not all of the NO_3^- anions have been exchanged by metanilic anions, and similar results have also been reported by other researchers in studies of the intercalation of large anions into NO_3-LDH precursors.[23,24] Furthermore, elemental analysis data show that the chemical composition of the NiAl-metanilic LDH is $Ni_{0.66}Al_{0.34}(OH)_2(C_6H_4NH_2SO_3)_{0.23}(NO_3)_{0.11}\cdot 0.78H_2O$, which is consistent with the results of XRD and IR spectroscopy.

The structure of an LDH is based on brucite-like layers in which octahedrally coordinated metal ions share edges to form infinite sheets.[25] The area of each $[Ni_{1-x}Al_x(OH)_2]^{x+}$ octahedral unit is related to the unit cell parameter a by the formula: $S = \sqrt{3}(a^2/2)$.[26] The value of a can be

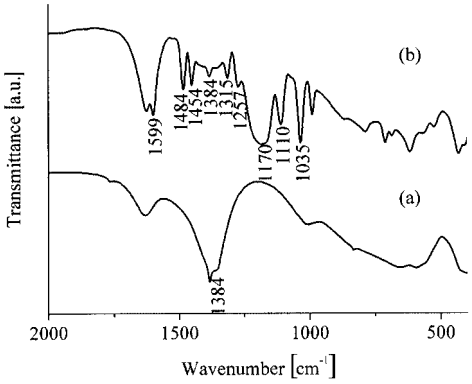

Figure 2. FT IR spectra for (a) NiAl-NO_3 LDH and (b) NiAl-metanilic LDH.

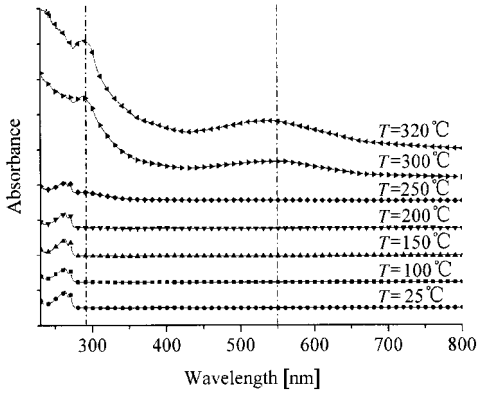

Figure 4. UV/Vis spectra of NiAl-metanilic LDH after heat treatment at different temperatures under nitrogen.

calculated from the XRD pattern in Figure 1b ($a = 2d_{110}$ = 2.99 Å). The area of each octahedral unit is therefore 7.74 Å^2, giving one positive charge per 23 Å^2 in the case of $x = 0.34$ (based on the chemical composition of NiAl-metanilic LDH given above). The maximum dimensions of the anion are calculated as 6–7 Å (calculated with Chemwin 6.0), and the corresponding cross-sectional area of the complex anions can thus be estimated to be in the range of 28–38 Å^2. Consequently, it is impossible for metanilic anions alone to balance the positive charge of the host layer, thereby accounting for the co-intercalation of NO_3^-.

On the basis of the discussion above, the structure of NiAl-metanilic LDHs can be represented as alternating NiAl-OH hydroxide layers and layers containing metanilic anions, NO_3^-, and water molecules. The schematic model of NiAl-metanilic LDHs is proposed in Figure 3.

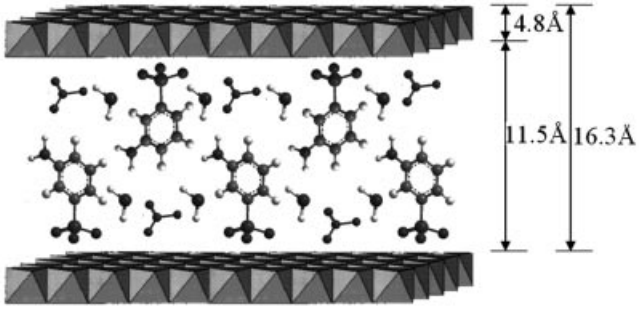

Figure 3. A schematic representation of the possible arrangement for NiAl-metanilic LDHs.

UV/Vis Spectroscopy

Results obtained by UV/Vis spectroscopy give evidence for the polymerization of metanilic anions intercalated in NiAl LDHs by heat treatment under nitrogen. Figure 4 shows the optical absorption spectra, in the wavelength range 230–800 nm, of the synthesized NiAl-metanilic LDH and the resultant products after heat treatment at different temperatures.

It can be seen from Figure 4 that two absorption bands at 262 and 269 nm at room temperature are observed, which are associated with the phenyl group of the metanilic monomer. Along with the heat treatment, a strong absorption band (centered at 296 nm) corresponding to the π_B–π_B* transition appears when the temperature reaches 300 °C,[27] indicating that the polymerization of the intercalated monomer occurrs and the polymeric product possesses alternative benzenoid units (see structure A). The absorption band centered at 550 nm, attributable to charge transfer from the benzoid to the quinoid segments (π_B–π_Q*), becomes more obvious when the temperature increases to 320 °C (see structures B and C).[28] The π_B–π_Q* transition provides direct evidence that quinoid units are produced and the interlayer polyaniline sulfonic (PANIS) is present in its highly oxidized form. This result is consistent with reports on the study, by optical absorption spectroscopy, of the interconversion of polyaniline oxidation states.[27,29,30]

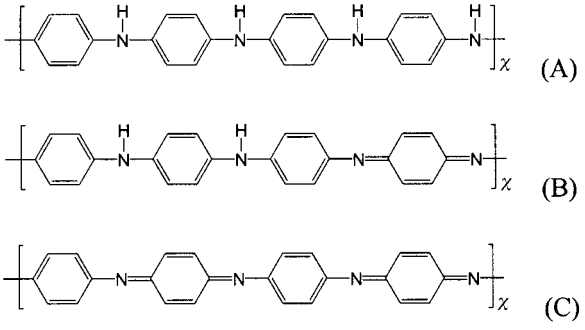

In Situ XANES

Previous studies on PANI/CuCr LDH nanocomposites show that oxidative Cu^{2+} has been used to induce the reaction of the oxidative polymerization of aniline in the interlayer galleries of pillared hosts.[14] In order to study whether Ni^{2+} in the host layer participates in the interlayer polymerization in this system, in situ X-ray absorption near edge structure (XANES) measurements were carried out at the Ni *K*-edge. The features in the absorption edge are sensitive

to the immediate Ni environment and local geometry. For the *K* edge, the existence of a pre-edge and its intensity are closely related to the degree of d–p orbital mixing, and loss of centrosymmetry can cause a large intensity of this peak. The dominant jump at the edge arises from the dipolar-allowed transition related to final electronic 4p states. Therefore, it is sensitive to the variation of the oxidation state of Ni.[31]

Figure 5 shows the normalized XANES spectra at the Ni *K*-edge of NiAl-metanilic LDH heated under nitrogen. The pre-edge peak (A) can be observed and this arises from the quadrupolar 1s→3d transition, which is directly related to the occupation of the 3d orbital and to the local symmetry. Peak C reflects the long-range ordering of the Ni–O or Ni–Ni shell.[32] During the heat treatment, a broadening of both peaks B and C was observed as a result of the thermal disorder. However, no significant shifts in the three peaks could be observed, implying that no dramatic redox process involving Ni occurred during the heat treatment. The results therefore demonstrate that Ni^{2+} in the host layer does not serve as the oxidant for the interlayer oxidative polymerization and thus maintains the same valence in the temperature range 25–320 °C.

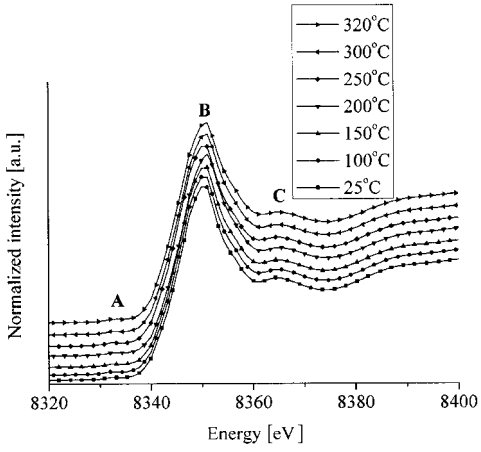

Figure 5. In situ XANES spectra at the Ni *K*-edge of NiAl-metanilic LDH heated from 25 to 320 °C under nitrogen.

TG–DTA–MS Analyses

Simultaneous thermogravimetric (TG) and–differential thermal analyses (DTA) combined with analysis by mass spectrometry was found to be useful for following the in situ thermal behavior of the organic/inorganic nanocomposites over a wide temperature range.[33]

The TG, DTG, and DTA profiles for the pristine metanilic acid are shown in Figure 6. It can be seen that metanilic acid exhibits rather high thermal stability from room temperature to 400 °C under nitrogen. Two consecutive weight losses occur between 400 and 500 °C, with two corresponding strong endothermic peaks in the DTA curve attributable to the decomposition of metanilic anions.

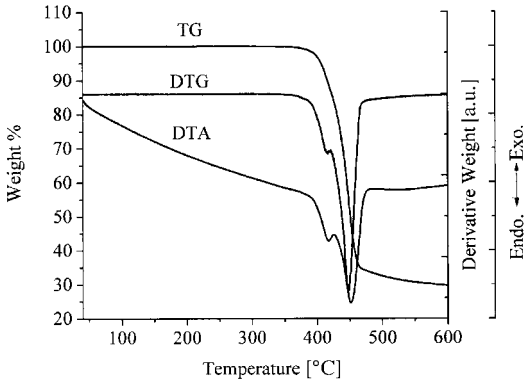

Figure 6. TG–DTA profiles of the pristine metanilic acid heated under nitrogen.

In the case of NiAl-metanilic LDH (Figure 7), the TG–DTA–MS determination shows that the thermal behavior under nitrogen can basically be described in four steps: the first step is observed between ambient temperature to about 100 °C. The TG curve displays a small weight loss with an endothermic peak in the DTA curve, and the corresponding MS determination (Figure 8 and Table 1) reveals one H_2O^+ (m/z = 18) peak at ca. 100 °C. This process is associated with the volatilization of the adsorbed water in the composite.

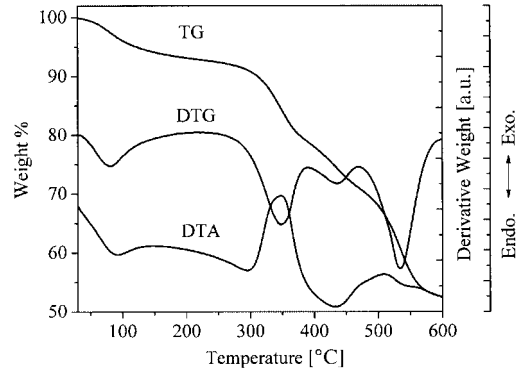

Figure 7. TG–DTA profiles of NiAl-metanilic LDH heated under nitrogen.

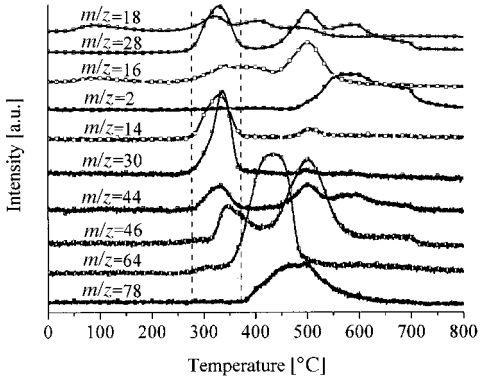

Figure 8. Mass analyses of NiAl-metanilic LDH heated under helium.

Table 1. Results for MS analyses of NiAl-metanilic LDH.

Proposed positive ion	H_2^+	N^+	O^+	H_2O^+	N_2^+	NO^+	N_2O^+	NO_2^+	SO_2^+	$C_6H_4^+$
m/*z*	2	14	16	18	28	30	44	46	64	76
Intensity [A]	10^{-11}	10^{-11}	10^{-11}	10^{-10}	10^{-10}	10^{-11}	10^{-11}	10^{-12}	10^{-12}	10^{-13}

The second step takes place in the temperature range 300–350 °C. The TG curve shows a big weight loss accompanied by a strong exothermic peak in the DTA curve. Several fragments assigned to N_2^+ (*m*/*z* = 28), NO^+ (*m*/*z* = 30), N_2O^+ (*m*/*z* = 44), H_2O^+ (*m*/*z* = 18), and NO_2^+ (*m*/*z* = 46) appear in the corresponding MS curves. For the nitrate-containing LDHs, the release of NO_2 and NO was generally attributable to the pyrolysis of nitrates, whereas the interlayer nitrate would be evolved as NO and N_2O only during the TPR experiment under hydrogen.[34] In this work, the release of N_2, NO, and N_2O at the same time provides evidence that the co-intercalated nitrate anions are involved in an interlayer redox reaction. The NO_2^+ peak lags behind the N_2^+, NO^+, N_2O^+, and H_2O^+ peaks, indicating that pyrolysis of the pre-intercalated nitrates occurs after reduction. The DTA curve in this step displays a strong exothermic peak at about 320 °C, which was not found in the DTA curve of the pristine metanilic acid. Roland-Swanson et al. have reported DTA traces with such an exothermic peak assigned to the polymerization of the 3-sulfopropyl methacrylate potassium salt (SPMA) intercalated in ZnAl LDHs by thermal treatment.[35] Because the reaction was complete without the use of any external chemical agent, the polymerization process was interpreted as an oxidative reaction induced by atmospheric oxygen. In the present study, this strong exothermic peak and the reduction of the co-intercalated nitrates correspond to the emergence of the new absorption bands attributable to the π_B–π_B* and π_B–π_Q* transitions in UV/Vis spectra, which demonstrates the polymerization of metanilic anions intercalated NiAl LDHs in the same temperature range. On the basis of the discussion above and of the comparison with other studies on the thermal behavior of the polymeric monomer/LDH nanocomposites, the strong exothermic process under an inert atmosphere in this work can be assigned to the chemical oxidative polymerization of the interlayer monomer with the co-intercalated nitrates acting as the oxidizing agent. This will be further discussed in the next sections.

The third weight loss (350–450 °C) is due to the pyrolysis of the hydroxide layers and the interlayer organic materials, which results in an enhanced signal of H_2O^+ (*m*/*z* = 18) and SO_2^+ (*m*/*z* = 64). The corresponding endothermic peak is observed at ca. 430 °C. The complete thermal decomposition of the nanocomposite occurs in the fourth step (450–600 °C).

In Situ FTIR

Figure 9 shows the in situ FTIR spectra for NiAl-metanilic LDH heated to different scheduled temperatures under nitrogen. Table 2 summarizes the assignments of the IR absorption bands for metanilic-intercalated LDH and its thermal products.[36,37]

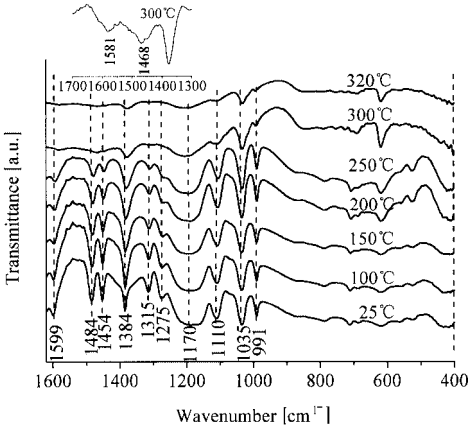

Figure 9. In situ FTIR spectra for the thermal polymerization of NiAl-metanilic LDH.

Table 2. Assignments for IR absorption bands for metanilic-intercalated LDH and its thermal products.[a]

Frequency [cm^{-1}]	Assignment
1599	disorder-induced C–C ring stretching
1581	stretching of N=Q=N
1484	ring stretching of C=C
1468	stretching of N=B=N
1453	stretching of benzene ring
1315	N–H in or out of plane bending
1275	C–H bending or C–N stretching
1170	C–H bending in plane
1110	C–S bending in plane
1035	S=O bending
991	C–H bending out of plane

[a] Abbreviations: B, benzenoid unit; Q, quinonoid unit.

It can be seen that very little change is observed for the three strong bands at 1599, 1484, and 1454 cm^{-1} and the weak band at 1315 cm^{-1}, which are characteristic absorptions of metanilic anions from room temperature to 250 °C. When the temperature increases to 300 °C, the former four characteristic bands weaken remarkably because of the increase in the conjugated degree of the polymerization products upon thermal treatment. Moreover, the emergence of the bands at 1581 and 1468 cm^{-1} in the spectrum of NiAl-metanilic LDH at 300 °C indicates that the polymerization product is in a high oxidation state.[38] The comparison of the IR spectrum of the original metanilic-intercalated LDH and those of its oxidation products after treatment at 300 °C reveals a sharp decrease in the intensity of the bands at 1170 (υ_{C-H} in plane), 1275, and 1315 cm^{-1}, which points to a substantial decrease in the number of amino groups ($-NH_2$). This further confirms the formation of an interlayer polyconjugated system. Moreover, the intensity of the band at 1384 cm^{-1} attributable to cointercalated NO_3^- decreases sharply as the temperature reaches 300 °C, thereby giving evidence that NO_3^- is engaged in the interlayer redox reaction. This is in agreement with the results of UV/Vis spectroscopy and TG–MS.

In Situ HT-XRD

In order to get further insight into the thermal polymerization process of the monomer intercalated NiAl LDH, in situ X-ray measurements were carried out. The temperatures at which the X-ray data were collected were defined on the basis of TG–DTA analysis. The in situ HT-XRD patterns of the intercalation product NiAl-metanilic LDH in the temperature range 25–320 °C under nitrogen are shown in Figure 10. The variation in the d_{003} basal spacing of NiAl-metanilic LDH with temperature is displayed in Figure 11.

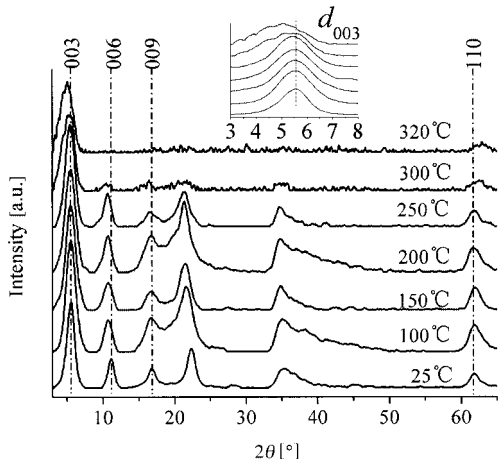

Figure 10. In situ HT-XRD patterns of NiAl-metanilic LDH in the temperature range 25–320 °C.

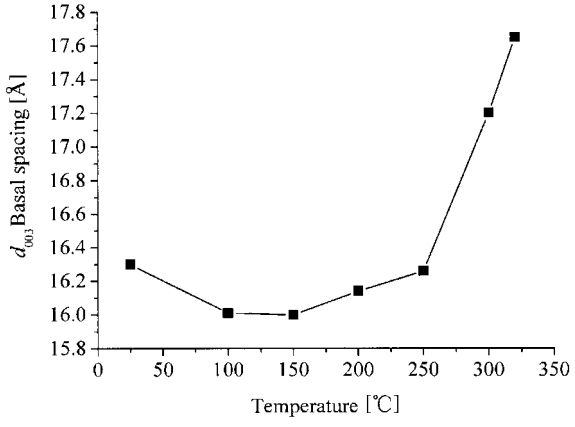

Figure 11. The relationship between the d_{003} basal spacing and temperature.

Upon increasing the temperature, the (003), (006), and (009) reflections of NiAl-metanilic LDH move to a slightly higher 2θ angle (as shown in Figure 10), and the (003) basal spacing decreases from 16.3 to 16.0 Å (Figure 11) when the material was heated from 25 °C to 150 °C. This contraction may result from the loss of absorbed water and parts of gallery water.[39] However, the value of d_{003} slowly increases from 16.0 Å at 150 °C to 16.2 Å at 250 °C. This might be due to the reorientation of the interlayer monomer accompanied by the loss of the gallery water.

When the temperature reaches 300 °C, the (003) reflection of the nanocomposite becomes broader and moves to a remarkably lower 2θ angle. The interlayer distance increases drastically from 16.2 Å at 250 °C to 17.2 Å at 300 °C, indicating that interlayer polymerization of the interlamellar species occurs. This phenomenon was also observed in the case of post-intercalative polymerization of aniline and its derivatives in layered metal phosphates after thermal treatment at 130 °C in air.[11] In addition, the color of the nanocomposite turns from bright green to dark brown after the heat treatment. The broadening of the (003) reflection and the decrease in intensity of other diffraction peaks of the nanocomposite at 300 °C indicate the decrease in ordered stacking sequences and in crystallinity during the polymerization process. Nevertheless, the diffraction maximum between the 2θ values of 62 and 63° (the spectrum at 300 °C in Figure 10) can still be observed, indicating the conservation of the lamellar structure with no substantial structural collapse during the interlayer polymerization reaction.

The coupling between the monomers and the arrangement of their subsequent dimerization or polymerization have been discussed in term of the gap sizes, which can be calculated by using the peak fit program of XRD-6000 Version 4.1.[17] The geometry and atomic charges of the possible dimers have been optimized by using the MOPAC semi-empirical method, employing the PM3 Hamiltonian.[40]

Figure 12 shows the peak fit results of d_{003} at 300 °C, at which the interlayer polymerization occurs. Three different d_{003} values, i.e. 15.77, 17.48, and 20.07 Å were obtained in this case, and the corresponding gallery heights were calculated to be 10.97, 12.68, and 15.27 Å, respectively, by subtracting the inorganic layer thickness of 4.8 Å. The polymerization between monomers located on different layers (opposite inner side) may proceed iso- or syndiotactically, and the coupling between monomers may occur by a linkage (α,β), (β,β), or (N,N). The calculated lengths of the three possible dimers are 10.43, 11.63, and 12.42 Å (as shown in Scheme 1), respectively. It can be concluded that the coupling between monomers most likely occurs by the linkages (α,β) and (N,N) since the calculated lengths of the two possible dimers (10.43 and 12.42 Å) correspond well with the two gallery heights of 10.97 and 12.68 Å. As a result, the coupling between monomers on different layers hereinbefore should give rise to the quasi-monolayer arrangement by the linkage (α,β) (Figure 13a), whereas the gallery height of 15.27 Å may result from the bilayer arrangement when polymerization occurs between the two monomers on the same layer (Figure 13b).[17] The linkage of N and N charac-

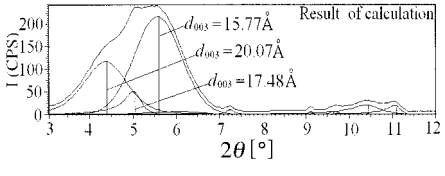

Figure 12. The peak fit results of d_{003} of NiAl-metanilic LDH at 300 °C.

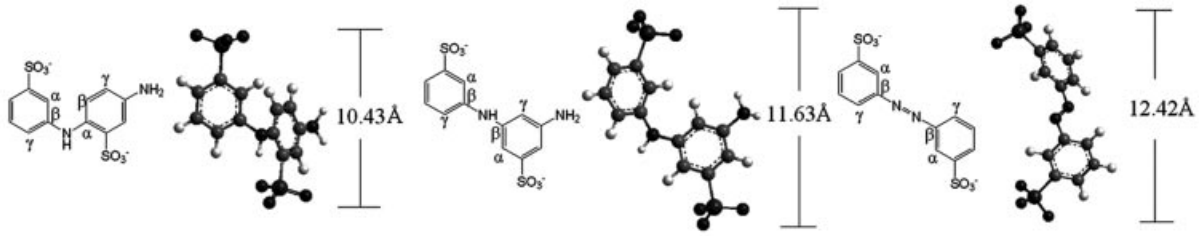

Scheme 1. The structure for the three possible dimers of metanilic anions formed by different linkages: (a) (α,β), (b) (β,β), and (c) (N,N).

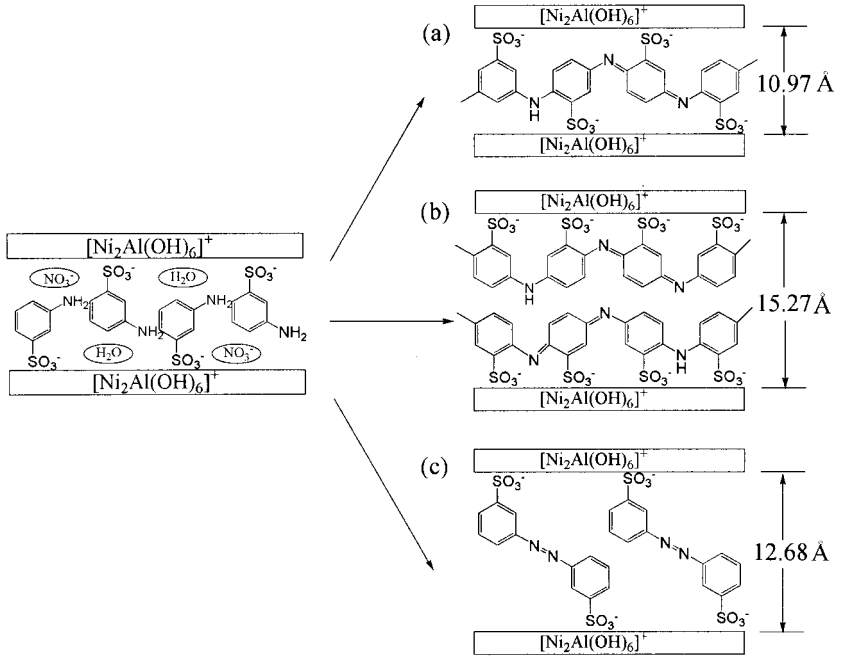

Figure 13. Schematic representations of the interlayer polymerization products.

teristics, which results from the "head-to-head" coupling (Figure 13c), was observed only in the spectra of products prepared under neutral or basic conditions. For instance, the formation of azobenzene derivatives in basic or in an acetonitrile/pyridine medium has also been reported by Wawzonek and MacIntyre.[41] On the basis of the discussion above, it can be concluded that the coupling between monomers most likely occurs by the (α,β) and (N,N) linkages, and the main coupling likely occurs by an (α,β) linkage. This is in agreement with the much earlier work of Mohilner et al., in which aniline oxidation products obtained in neutral or weakly acidic media have a predominantly "head-to-tail" arrangement.[42]

TEM

The TEM micrographs of the prepared materials are illustrated in Figure 14. It can be seen that NiAl-metanilic LDH exhibits the characteristic LDH platelet, an ill-defined shape with a uniform size from 200 to 300 Å (Figure 14a). This morphological result is consistent with that from HT-XRD analysis. The polymerization product PANIS shows a similar platelike morphology (Figure 14b) with average particle size of 50–100 Å. Such a small size is possibly due to the restriction on the chain growth of PANIS afforded by the layers of LDH.

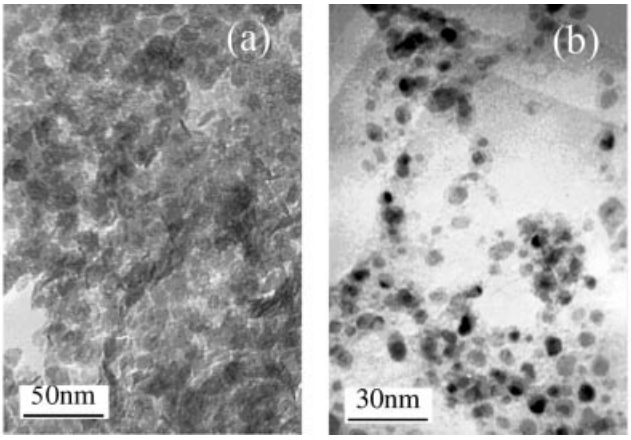

Figure 14. TEM images of (a) NiAl-metanilic LDH and (b) the polymerization product (PANIS).

Conclusions

The in situ chemical oxidative polymerization of metanilic anions (m-$NH_2C_6H_4SO_3^-$) intercalated in NiAl LDH has been performed for the first time by the use of pre-intercalated nitrate as the oxidizing agent. From the characterization by XRD, IR spectroscopy, elemental analysis, and geometrical considerations, the schematic model of NiAl-metanilic LDH has been proposed in which the structure can be represented as alternating NiAl-OH hydroxide layers and layers containing metanilic anions, NO_3^- ions, and water molecules.

Results obtained by UV/Vis spectroscopy give evidence for the polymerization of the metanilic anions intercalated NiAl LDH when the temperature reaches 300 °C. The particle sizes of 50–100 Å of the interlayer polymerization product determined by TEM microscopy indicates the low conjugation extent of the interlayer PANIS.

In situ XANES demonstrates that Ni^{2+} in the host layer does not serve as the oxidant for interlayer oxidative polymerization. According to the results of TG–DTA–MS for the pristine metanilic acid and the NiAl-metanilic LDH under nitrogen, we propose that the pre-intercalated nitrate anions act as the oxidant, which induces the polymerization of the interlayer monomer under nitrogen upon heating at 300 °C.

In situ FTIR and in situ HT-XRD provide further insight into the thermal polymerization process. The basal spacing increases from 16.0 to 17.2 Å, and the characteristic vibrational absorptions of polyaniline emerge at 300 °C under nitrogen. It can be concluded, on the basis of the peak fit program and the MOPAC semi-empirical method, that the coupling between monomers most likely occurs by the (α,β) and (N,N) linkages. The possible schematic arrangement for the interlayer products has also been proposed.

Experimental Section

Reagents: All chemicals used in this synthesis including $Ni(NO_3)_2{\cdot}6H_2O$, $Al(NO_3)_3{\cdot}9H_2O$, NaOH, and metanilic acid (m-$NH_2C_6H_4SO_3^-$) were of analytical grade and were purchased from Aldrich and used without any further purification. High purity nitrogen gas ($O_2 < 1$ ppm) and high purity helium gas ($O_2 < 1$ ppm) were purchased from the Beijing Chemical Plant Limited. All solutions were prepared with distilled and decarbonated water.

Synthesis: The precursor LDH $[Ni_2Al(OH)_6(NO_3)]{\cdot}nH_2O$ was prepared following a standard aqueous coprecipitation and thermal crystallization method.[18] A solution of NaOH (8.0 g, 0.20 mol) in water (100 mL) was added dropwise over 2 h to a solution (100 mL) containing $Ni(NO_3)_2{\cdot}6H_2O$ (19.4 g, 0.066 mol) and $Al(NO_3)_3{\cdot}9H_2O$ (12.5 g, 0.033 mol), with vigorous stirring under nitrogen. The pH value of the solution at the end of addition was 7.0. The resultant gelatinous precipitate was maintained at 100 °C for 72 h, centrifuged, and washed thoroughly with water before drying at 70 °C for 24 h under vacuum.

The metanilic intercalated NiAl-LDH was prepared following the ion-exchange method. A solution (100 mL) of metanilic acid (10.4 g, 6.0 mmol) with a pH value adjusted to 7.0 using NaOH (2.0 M) was added to a suspension of NiAl-NO_3 LDH (5.0 g, *ca.* 1.5 mmol) in water (100 mL). The mixture was held at 30 °C under nitrogen for 72 h. The product was washed extensively with water, centrifuged, and dried under vacuum for 24 h.

For the thermal treatment, the hybrid phase was placed in a tube furnace heated at 25, 100, 150, 200, 250, 300, or 320 °C for 0.5 h under nitrogen.

Characterization Techniques: Powder X-ray diffraction (XRD) measurements were performed on a Rigaku XRD-6000 diffractometer, using Cu-K_α radiation (λ = 1.5418 Å) at 40 kV and 30 mA. Data were collected over the angular range of 2θ from 3° to 70° at a scanning rate of 0.02° per second at room temperature. The UV/Vis spectra were collected in reflectance mode using a Shimadzu UV-2401 spectrophotometer in the 230–800 nm region (the samples were dissolved in 0.1 M hydrochloric acid). Fourier transform infrared (FTIR) spectra were recorded using a Vector 22 (Bruker) spectrophotometer in the range 4000 to 400 cm^{-1} with 2 cm^{-1} resolution. The standard KBr disk (1 mg of sample in 100 mg of KBr) was used. In situ XANES spectra were collected at the XAFS station (beam line 4W1B) of the Beijing Synchrotron Radiation Facility. The storage ring energy was 2.2 GeV and the current was 50–60 mA. The X-rays were monochromated by using a Si (111) single crystal. Samples were shaped into ingots with a thickness of about 1 mm. X-ray absorption spectra of the Ni K-edge were collected at ambient temperature up to 320 °C with a heating rate of 5 °C min^{-1} under nitrogen in the transmission mode. The incident and transmission X-ray intensities were detected using ion chambers which were installed in front of and behind the sample, respectively. In situ HT-XRD measurements were performed on a Rigaku D/max 2500VB2+/PC diffractometer in the temperature range 25–320 °C under nitrogen by using Cu-K_α radiation (λ = 1.5418 Å) at 40 kV and 30 mA. The samples as disoriented powders were scanned in steps of 0.02° in the 2θ range 3°–70° by using a count time of 4 s per step. An α-Al_2O_3 substrate was used. In situ FTIR spectra were recorded with a Nicolet 60sxb spectrometer in the range 4000 to 400 cm^{-1} with 2 cm^{-1} resolution. The spectra were obtained every 10° with a heating rate of 5 °C min^{-1} under nitrogen. The standard KBr disk method (1 mg of sample in 100 mg of KBr) was used. TG–DTA analyses were carried out under nitrogen (flux of 100 mL min^{-1}) with a Seiko 6300 simultaneous DTA–TGA apparatus from Seiko Instruments, at a heating rate of 5 °C min^{-1}, with Al_2O_3 as a reference. Simultaneous TG–MS analyses were performed with a Pyris Diamond TG–DTA instrument coupled to a ThermoStar™ QM220 mass spectrometer by a quartz capillary transfer line at 180 °C. The heating rate was 5 °C min^{-1}, with a helium flow of 100 mL min^{-1}. The scanning speed of mass was 1 a.m.u s^{-1}, with a filtering time 0.03 s. The TGA apparatus operated at atmospheric pressure, and the mass spectrometer at a working pressure of 3×10^{-6} mPa and an electron energy of 70 eV. The proposed mass number, the ion current intensity, and the amplifying rate are listed in Table 1. Elemental analyses were performed with a Shimadzu ICPS-7500 instrument. C, H, and N content were determined by using an Elementarvario elemental analysis instrument. TEM images were obtained by using a JEOL JEM-1200 instrument operating at an acceleration voltage of 80 kV. The TEM samples were ultrasonically dispersed in water, and then a suspension was deposited onto a holey carbon film deposited on a Cu grid.

Acknowledgments

This project was supported by the National Natural Science Foundation Key Project of China (Project No.: 20531010), the National

Natural Science Foundation Major International Joint Research Program (Project No.: 20620130108), the Beijing Nova Program (No.: 2004A13), and the Program for Changjiang Scholars and the Innovative Research Team at the University (PCSIRT). We also acknowledge the Beijing Synchrotron Radiation Facility (BSRF) for provision of synchrotron radiation facilities and thank Dr. Tao Liu and Yaning Xie for assistance in using beamline 4W1B.

[1] A. I. Khan, D. O'Hare, *J. Mater. Chem.* **2002**, *12*, 3191–3198.
[2] F. Leroux, J. P. Besse, *Chem. Mater.* **2001**, *13*, 3507–3515.
[3] R. Schollhorn, *Chem. Mater.* **1996**, *8*, 1747–1757.
[4] L. Vieille, E. M. Moujahid, C. Taviot-Guého, J. Cellier, J. P. Besse, F. Leroux, *J. Phys. Chem. Solids* **2004**, *65*, 385–393.
[5] E. M. Moujahid, F. Leroux, M. Dubois, J. P. Besse, *C. R. Chim.* **2003**, *6*, 259–264.
[6] M. G. Kanatzidis, C. G. Wu, H. O. Marcy, C. R. Kannewurf, *J. Am. Chem. Soc.* **1989**, *111*, 4139–4141.
[7] T. A. Kerr, H. Wu, L. F. Nazar, *Chem. Mater.* **1996**, *8*, 2005–2015.
[8] P. Liu, K. Gong, *Carbon* **1999**, *37*, 706–707.
[9] L. Wang, P. Brazis, M. Rocci, C. R. Kannewurf, M. G. Kanatzidis, *Chem. Mater.* **1998**, *10*, 3298–3300.
[10] H. Inoue, H. J. Yoneyama, *J. Electroanal. Chem.* **1987**, *233*, 291–294.
[11] Y. J. Liu, M. G. Kanatzidis, *Chem. Mater.* **1995**, *7*, 1525–1533.
[12] C. B. Koch, *Hyperfine Interact.* **1998**, *117*, 131–157.
[13] F. Cavani, F. Trifiro, A. Vaccari, *Catal. Today* **1991**, *11*, 173–301.
[14] T. Challier, R. C. T. Slade, *J. Mater. Chem.* **1994**, *4*, 367–371.
[15] E. M. Moujahid, M. Dubois, J. P. Besse, F. Leroux, *Chem. Mater.* **2002**, *14*, 3799–3807.
[16] V. P. Isupov, L. E. Chupakhina, M. A. Ozerova, V. G. Kostrovsky, V. A. Poluboyarov, *Solid State Ionics* **2001**, *141–142*, 231–236.
[17] E. M. Moujahid, M. Dubois, J. P. Besse, F. Leroux, *Chem. Mater.* **2005**, *17*, 373–382.
[18] J. Wilson, T. Olorunyolemi, A. Jaworski, L. Borum, D. Young, A. Siriwat, E. Dickens, *Appl. Clay Sci.* **1999**, *15*, 265–279.
[19] N. T. Whilton, P. J. Vickers, S. Mann, *J. Mater. Chem.* **1997**, *7*, 1623–1629.
[20] F. Prinetto, D. Tichit, R. Teissier, B. Coq, *Catal. Today* **2000**, *55*, 103–116.
[21] J. Zhang, F. Z. Zhang, L. L. Ren, D. G. Evans, X. Duan, *Mater. Chem. Phys.* **2004**, *85*, 207–214.
[22] T. A. Huber, *A Literature Survey of Polyaniline*, Defence R&D Canada – Atlantic, **2003**, p. 014.
[23] N. T. Whilton, P. J. Vickers, S. Mann, *J. Mater. Chem.* **1997**, *7*, 1623–1629.
[24] A. Fudala, I. Palinko, I. Kiricsi, *Inorg. Chem.* **1999**, *38*, 4653–4658.
[25] G. W. Brindley, S. Kikkawa, *Am. Mineral.* **1979**, *64*, 836–843.
[26] S. K. Yun, T. J. Pinnavaia, *Chem. Mater.* **1995**, *7*, 348–354.
[27] J. E. de Albuquerque, L. H. C. Mattoso, M. Faria, J. G. Masters, A. G. MacDiarmid, *Synth. Met.* **2004**, *146*, 1–10.
[28] B. A. Deore, I. Yu, M. S. Freund, *J. Am. Chem. Soc.* **2004**, *126*, 52–53.
[29] V. Luca, S. Thomson, *J. Mater. Chem.* **2000**, *10*, 2121–2126.
[30] L. W. Shacklette, J. F. Wolf, S. Gould, R. H. Baughman, *J. Chem. Phys.* **1988**, *88*, 3955–3961.
[31] F. Leroux, P. J. Dewar, M. Intissar, G. Ouvrard, L. F. Nazar, *J. Mater. Chem.* **2002**, *12*, 3245–3253.
[32] M. Jiménez-Ruiz, C. Prieto, J. L. Martínez, J. M. Alonso, *J. Solid State Chem.* **1998**, *140*, 278–284.
[33] C. W. Lu, Z. He, T. G. Xi, Y. X. Chen, L. Luo, *Thermochim. Acta* **1999**, *334*, 149–155.
[34] D. Tichit, F. Medina, B. Coq, R. Dutartre, *Appl. Catal. A* **1997**, *159*, 241–258.
[35] C. Roland-Swanson, J. P. Besse, F. Leroux, *Chem. Mater.* **2004**, *16*, 5512–5517.
[36] M. C. Miras, C. Barbero, O. Haas, *Synth. Met.* **1991**, *43*, 3081–3084.
[37] Y. Furukawa, F. Ueda, Y. Hyodo, I. Harada, T. Nakajima, T. Kawagoe, *Macromolecules* **1988**, *21*, 1297–1305.
[38] E. T. Kang, K. G. Neoh, K. L. Tan, *Prog. Polym. Sci.* **1998**, *23*, 277–324.
[39] M. Wei, J. Wang, J. He, D. G. Evans, X. Duan, *Microporous Mesoporous Mater.* **2005**, *78*, 53–61.
[40] A. M. Aicken, I. S. Bell, P. V. Coveney, W. Jones, *Adv. Mater.* **1997**, *9*, 496–500.
[41] S. Wawzonek, T. W. MacIntyre, *J. Electrochem. Soc.* **1972**, *119*, 1350–1357.
[42] D. M. Mohilner, R. N. Adams, W. J. Argersinger, *J. Am. Chem. Soc.* **1962**, *84*, 3618–3622.

Received: March 9, 2006
Published Online: July 11, 2006

